

This article was downloaded by: [Tomsk State University of Control Systems and Radio]

On: 20 February 2013, At: 12:03

Publisher: Taylor & Francis

Informa Ltd Registered in England and Wales Registered Number: 1072954

Registered office: Mortimer House, 37-41 Mortimer Street, London W1T 3JH, UK



## Molecular Crystals and Liquid Crystals

Publication details, including instructions for authors and subscription information:

<http://www.tandfonline.com/loi/gmcl16>

### Polar Alkenyls: Physical Properties and Correlations with Molecular Structure of New Nematic Liquid Crystalsf

M. Schadt<sup>a</sup>, M. Petrzilka<sup>a</sup>, P. R. Gerber<sup>a</sup> & A. Villiger<sup>a</sup>

<sup>a</sup> Central Research Units, F. Hoffmann-La Roche & Co. Ltd., CH-4002, Basel, Switzerland

Version of record first published: 17 Oct 2011.

To cite this article: M. Schadt, M. Petrzilka, P. R. Gerber & A. Villiger (1985): Polar Alkenyls: Physical Properties and Correlations with Molecular Structure of New Nematic Liquid Crystalsf, *Molecular Crystals and Liquid Crystals*, 122:1, 241-260

To link to this article: <http://dx.doi.org/10.1080/00268948508074756>

PLEASE SCROLL DOWN FOR ARTICLE

Full terms and conditions of use: <http://www.tandfonline.com/page/terms-and-conditions>

This article may be used for research, teaching, and private study purposes. Any substantial or systematic reproduction, redistribution, reselling, loan, sub-licensing, systematic supply, or distribution in any form to anyone is expressly forbidden.

The publisher does not give any warranty express or implied or make any representation that the contents will be complete or accurate or up to date. The accuracy of any instructions, formulae, and drug doses should be

independently verified with primary sources. The publisher shall not be liable for any loss, actions, claims, proceedings, demand, or costs or damages whatsoever or howsoever caused arising directly or indirectly in connection with or arising out of the use of this material.

# Polar Alkenyls: Physical Properties and Correlations with Molecular Structure of New Nematic Liquid Crystals†

M. SCHADT, M. PETRZILKA, P. R. GERBER and A. VILLIGER

*Central Research Units, F. Hoffmann-La Roche & Co. Ltd.,  
CH-4002 Basel/Switzerland*

*(Received July 19, 1984)*

The elastic constants  $k_{11}$ ,  $k_{22}$ ,  $k_{33}$ , the bulk and rotational viscosities, the birefringence, the static dielectric and electro-optical properties in TN-LCDs of new, positive dielectric and electro-optical properties in TN-LCDs of new, positive dielectric nematic liquid crystals, namely polar alkenyls, are reported. The molecules comprise a double bond in their hydrocarbon side chain as well as different rigid cores, namely directly- and ethane linked PCH-cores as well as heterocyclic (dioxane) cores. Despite their dielectric and conformational similarity, large variations of the elastic constants depending on the position of the alkenyl double bond are shown to result in alkenyls with PCH cores. This leads to variations of  $k_{33}/k_{11}$  and  $\kappa = k_{11} + (k_{33} - 2k_{22})/4$  among different alkenyls with the same chain length of almost a factor of 2 at constant reduced temperature ( $T_r$ -10°C). From molecular modelling follow rod-shaped van der Waals conformations with constant length/width ratio  $L/W$  for all directly linked alkenyls. Therefore, and due to  $k_{33}/k_{11} \neq \text{constant}$ , nematic hard-rod models neglecting molecule-specific interactions and implying  $k_{33}/k_{11} \propto L/W$  are qualitatively shown to be inadequate to explain the elastic ratios of nematics. Despite up to 30% larger optical anisotropies the response times of some alkenyls in TN-LCDs are  $\sim 30\%$  shorter than those of PCHs. This result is not primarily due to the low rotational viscosity  $\gamma_1$  of alkenyls but rather due to their low visco-elastic ratios  $\gamma_1/\kappa$ . The fast response and the wide range of elastic properties render the stable polar alkenyls applicable for highly multiplexed as well as fast responding LCDs.

## 1. INTRODUCTION

Polar nematic liquid crystals comprising molecules with structural elements leading to strong longitudinal permanent dipole moments

†Paper presented at the 10th International Liquid Crystal Conference, York, 15th-21st July 1984.

exhibit the positive dielectric anisotropy  $\Delta\epsilon = (\epsilon_{\parallel} - \epsilon_{\perp})$  that is required for most LCD applications. From correlations of material properties with molecular structures of polar and nonpolar representatives of the same liquid crystal class we found that polar groups not only determine  $\Delta\epsilon$  but also strongly affect the elastic constants and the viscosity of nematics. Thus, in structurally comparable liquid crystals the bend/splay elastic ratio  $k_{33}/k_{11}$  decreases within a given class when reducing the polarity and thus  $\Delta\epsilon$  of the molecules.<sup>1</sup> Moreover,  $k_{33}/k_{11}$  is affected by the type of ring structures of which the rigid part of the molecules consists.<sup>1</sup> As a consequence, and especially in cases where heterocyclic rings are involved, low elastic ratios  $k_{33}/k_{11}$  and therefore steep electro-optical characteristics in twisted nematic displays (TN-LCDs) can be achieved. Apart from  $\Delta\epsilon$  and specific structural elements,  $k_{33}/k_{11}$  of nematics is also affected by the number of carbon atoms in alkyl side chains. De Jeu *et al.* who investigated a homologous series of nonpolar azoxybenzenes found  $k_{33}/k_{11}$  to decrease with increasing chain length.<sup>2</sup> An analogous behaviour was reported<sup>3</sup> for polar phenylcyclohexanes<sup>4</sup> (PCHs). As the dielectric and elastic properties, the bulk viscosity  $\eta$ <sup>5,6</sup> as well as the rotational viscosity  $\gamma_1$ <sup>7</sup> are also affected by polar groups. Thus, nematics with  $\Delta\epsilon \gg 0$  exhibit in general considerably larger viscosities than their nonpolar counterparts.

Regrettably, there seem to be no theoretical model calculations in the literature extending mean-field theories as those of Maier and Saupe,<sup>8</sup> Priest<sup>9</sup> or Straley<sup>10</sup> which would take into account specific molecular interactions, i.e. induced dipole-dipole or permanent dipole interactions. From the calculations of Priest<sup>9</sup> and Straley<sup>10</sup> who included higher order terms in the intermolecular mean-field potential of the Onsager hard rod model which holds for extremely long rods, one is tempted to conclude<sup>11</sup> that  $k_{33}/k_{11}$  increases in nematics with increasing length to width ratio  $L/W$  of the (short) nematic rods and/or with increasing  $L/W$  ratio of hypothetical sterical units.<sup>19</sup> However, the above cited experiments<sup>1,2,3</sup> performed with dielectrically and structurally distinct but comparable classes indicate that geometrical considerations alone are inadequate to predict the important elastic ratios of nematic liquid crystals. Molecular-specific interactions have to be taken into account.

In the following the properties of five new polar nematic liquid crystal families with rather unusual elastic and viscous behaviour synthesized in our laboratories are presented, namely cyano alkenyls. The classes differ from each other with respect to the position of the alkenyl double bond in the hydrocarbon side chain and/or with

respect to their rigid core which consists either of a PCH ring system, an ethane linked ring system or a phenyl-dioxane ring system. The elastic ratio  $k_{33}/k_{11}$  as well as the elastic expression  $\kappa = k_{11} + (k_{33} - 2k_{22})/4$  of polar alkenyls are shown to depend strongly on the position of the double bond; i.e. on a seemingly minor structural modification. Moreover, their low rotational viscosities are also shown to depend on alkenyl position. From the low viscoelastic ratios  $\gamma_1/\kappa$  of some alkenyls, response times of TN-LCDs result which are up to 30% lower than those of the fast responding PCHs. We show that the large range over which  $k_{ii}$  of the dielectrically and sterically similar new compounds varies is incompatible with the constant  $L/W$  ratio of their rod shaped van der Waals radii determined with an interactive molecular graphics modelling system.

## 2. EXPERIMENTAL

### 2.1. Structures of nematics

The upper part of Table I depicts the cyano alkenyls chosen for our investigations. For comparison the lower part shows cyano compounds exhibiting the same rigid core as the alkenyls, namely PCHs,<sup>4</sup> ethanes<sup>12</sup> and dioxanes;<sup>14</sup> also included is a biphenyl.<sup>13</sup> To avoid effects caused by different hydrocarbon chain lengths, the chains of all individual components are identical, they comprise five carbon atoms. Table I shows three different PCH type alkenyls namely 3d<sub>1</sub>CP, 1d<sub>3</sub>CP and Ød<sub>4</sub>CP. The only difference among them lies in the position of the alkenyl bond  $d_x$  where  $x$  denominates the position of the double bond from the respective cyclohexane ring C (c.f. nomenclature in caption of Table I). For the investigation of monotropic or barely nematic compounds, binary mixtures were made of components whose number of chain carbon atoms differ by 1. To allow comparisons with earlier reported investigations<sup>1</sup> on other LC-classes molar proportions of (60/40) were used (Tab. I). The positional influence of the alkenyl double bond was investigated with mixtures  $m_1$ – $m_4$  exhibiting comparable nematic temperature ranges  $T_m \dots T_c$  (Tab. I).  $m_1$  comprises alkenyls in 1-position only, whereas  $m_2$  is a combination between position 1 and 3;  $m_3$  is a pure 3-alkenyl mixture and  $m_4$  combines position 1 with 4. The directly linked and the ethane linked 3-position alkenyl mixtures  $m_3$  and  $m_5$  are used to study the influence of the (flexible) ethane linkage on alkenyls.

TABLE I

Single components (100%) and binary mixtures (60% mol/40%) with their respective melting and nematic-isotropic transition temperatures  $T_m$  and  $T_c$ .

The following nomenclature is used for the structural elements:

C = cyclohexane ring, P = phenyl ring, B = biphenyl, D = dioxane ring, A = ethane linkage and  $d_x$  = alkenyl double bond with  $x$  defining its position in the chain (increasing  $x$  corresponds to a shift of the double bond away from the rigid core). The numbers in front of  $d_x$  are those of the carbon atoms attached to the double bond. In case of alkyl side chains they denominate the total number of carbon atoms in the chain.

COMPOSITION	MOL.PROP.	STRUCTURE	$T_m$ [°C]	$T_c$ [°C]	REF.
3d <sub>1</sub> CP	100%		16	58.5	
1d <sub>3</sub> CP	100%		60	73.7	n o v e l  l i q u i d  c r y s t a l s
8d <sub>4</sub> CP	100%		30	10.2	
3d <sub>1</sub> CAP	100%		25	47.5	
1d <sub>3</sub> CAP	100%		44	65.5	
m <sub>1</sub> = (3d <sub>1</sub> CP, 2d <sub>1</sub> CP)	(60,40)		<5	52.2	
m <sub>2</sub> = (3d <sub>1</sub> CP, 8d <sub>3</sub> CP)	(60,40)		<5	50.9	c r y s t a l s
m <sub>3</sub> = (1d <sub>3</sub> CP, 8d <sub>3</sub> CP)	(60,40)		38	65.2	
m <sub>4</sub> = (3d <sub>1</sub> CP, 8d <sub>4</sub> CP)	(60,40)		-5	35.1	
m <sub>5</sub> = (1d <sub>3</sub> CAP, 8d <sub>3</sub> CAP)	(60,40)		-25	57.7	
m <sub>6</sub> = (4d <sub>1</sub> DP, 3d <sub>1</sub> DP)	(60,40)		-35	45.3	
K15 (≅5B)	100%		24	34.8	[13]
PCH5 (≅5CP)	100%		30	54.8	[4]
5CAP	100%		31	52.5	[12]
m <sub>7</sub> = (4DP, 5DP)	(60,40)		-27	40.5	[14]

## 2.2. Dielectric, elastic and viscous properties of binary alkenyl mixtures

Figure 1 shows the temperature dependence of the static dielectric constants  $\epsilon_{\perp}$  and  $\Delta\epsilon$  of alkenyl mixtures  $m_1$ – $m_5$ . For comparison, measurements of the cyano biphenyl K15 are included. The results show—except for a more pronounced temperature dependence  $\Delta\epsilon(T)$  of  $m_4$  which approaches that of K15—no significant variations of either  $\epsilon_{\perp}$  or  $\Delta\epsilon$  among  $m_1$ – $m_5$ .

In Figure 2 the temperature dependences of the splay ( $k_{11}$ ) twist ( $k_{22}$ ) and bend ( $k_{33}$ ) elastic constants of mixtures  $m_1$ – $m_5$  are depicted. The lack of smectic pretransitional increases<sup>1</sup> of  $k_{ii}$  in Figure 2 with decreasing temperature proves that mixtures  $m_1$ – $m_5$  are indeed nematic in the temperature range studied. From Figure 2 follows that all three elastic constants strongly depend on the position of the alkenyl double bond. When shifting the double bond from position  $1 \rightarrow 3 \rightarrow 4$  the following order results:

$$k_{ii}(m_4) < k_{ii}(m_1) < k_{ii}(m_2) < k_{ii}(m_3) < k_{ii}(m_5).$$

Thus, a shift of the double bond from position  $1 \rightarrow 3$  causes  $k_{11}$ ,  $k_{22}$  and  $k_{33}$  to strongly increase. The increase is least pronounced for  $k_{22}$  and strongest for  $k_{33}$  (c.f.  $m_1$ – $m_3$  in Fig. 2). The incorporation of an ethane linkage in the rigid core of 3-alkenyls, further pronounces this

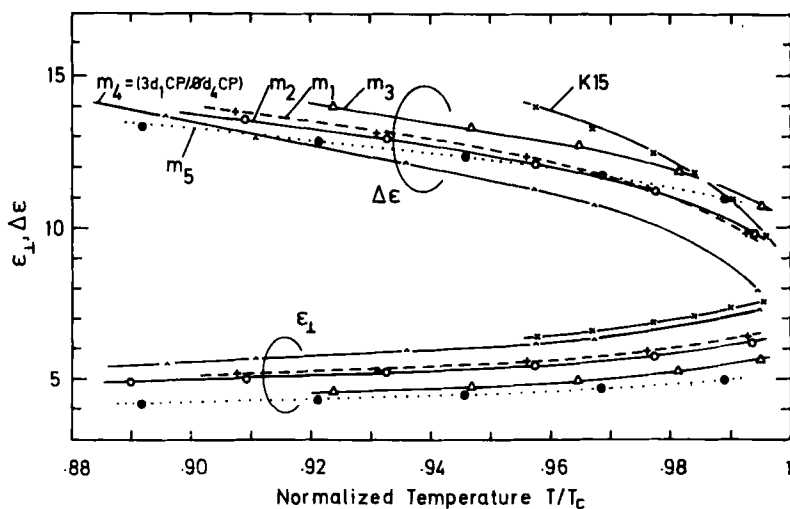


FIGURE 1 Temperature dependence of the static dielectric constants  $\epsilon_{\perp}$ ,  $\Delta\epsilon = (\epsilon_{\parallel} - \epsilon_{\perp})$  of alkenyl mixtures  $m_1$ – $m_5$  and of the biphenyl K15.

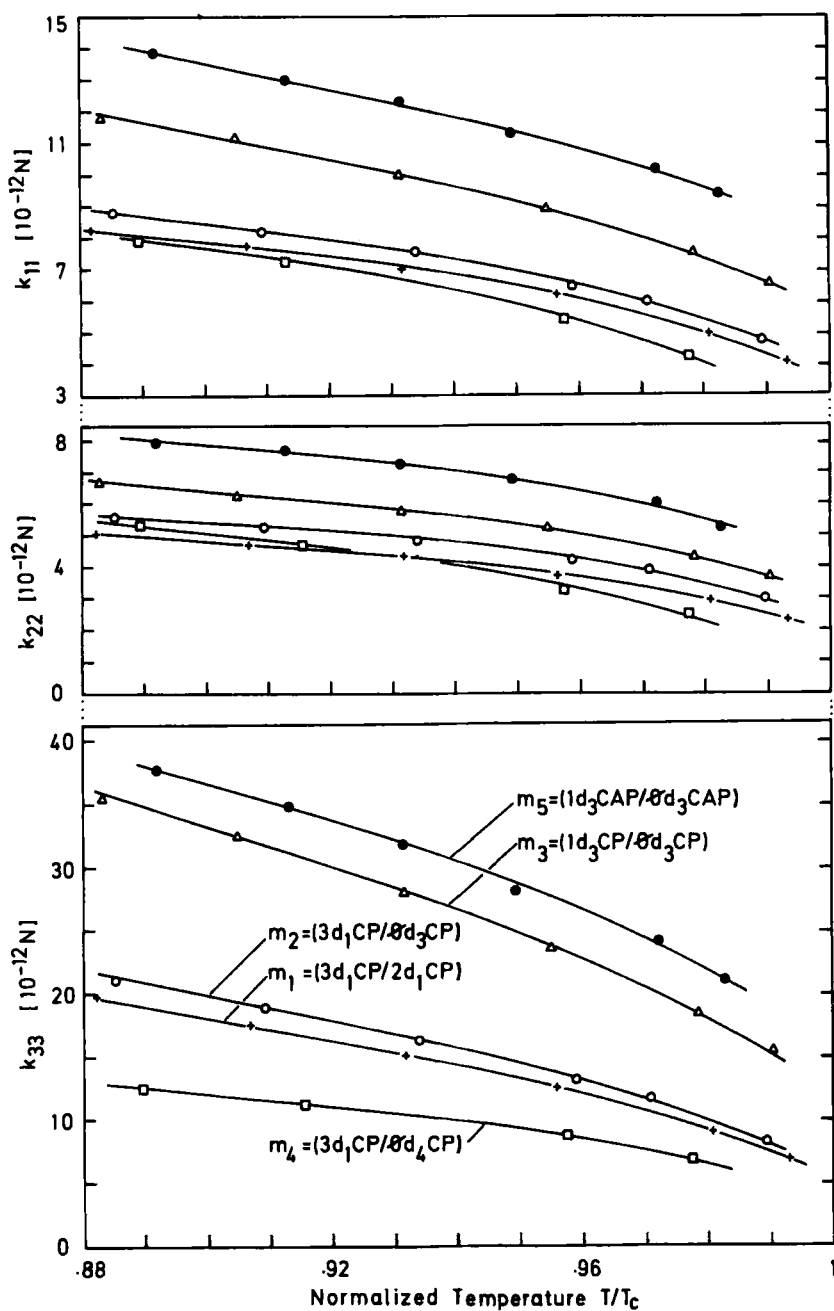


FIGURE 2 Temperature dependence of the splay ( $k_{11}$ ), twist ( $k_{22}$ ) and bend ( $k_{33}$ ) elastic constants of alkenyl mixtures  $m_1$ – $m_5$ .



trend (c.f.  $m_3$  and  $m_5$  in Fig. 2). On the other hand the results obtained for  $m_1$  and  $m_4$  in Figure 2 show that shifting the double bond from 1  $\rightarrow$  4 causes  $k_{ii}$  to strongly decrease. Preliminary experiments performed with monotropic 2-alkenyls indicate that position 2 affects  $k_{ii}$  similarly to position 4. The positional dependent variations of  $k_{33}$  that follow from Figure 2 for pentyl alkenyls exceed 300%. To our knowledge such a broad  $k_{ii}$ -range has so far not even been reached when comparing markedly different polar LC-classes<sup>1</sup> such as pyrimidines, PCHs, esters, Schiff bases, etc.

From Figure 2 follow two consequences which are important from a practical point of view as well as for a better understanding of structure-property relationships of nematics, namely: large variations of  $k_{33}/k_{11}$  and of  $\kappa = k_{11} + (k_{33} - 2k_{22})/4$ . This is shown in Figure 3 where the temperature dependences of  $k_{33}/k_{11}$  and of  $\kappa$  of mixtures  $m_1$ – $m_5$  are depicted. From Figure 3 follows that the elastic ratio  $k_{33}/k_{11}$  (i) increases when shifting the alkenyl double bond from 1  $\rightarrow$  3 (c.f.  $m_1$ ,  $m_2$ ,  $m_3$  and  $m_5$ ) and (ii) decreases for a 1  $\rightarrow$  4 shift (c.f.  $m_1$  and  $m_4$ ). Thus, for  $T \ll T_c$   $k_{33}/k_{11}$  varies between 1.5 and 3, i.e. by a factor of 2 (Fig. 3). The upper part of Figure 3 shows the analogous position-dependent behaviour of the elastic expression  $\kappa$ , i.e.  $\kappa$  increases by a factor of 2 when shifting the alkenyl double bond from position 1  $\rightarrow$  3 (c.f.  $m_1$ ,  $m_3$  and  $m_5$ ).

Figure 4 shows the temperature dependence of the rotational viscosities  $\gamma_1$  of mixtures  $m_1$ – $m_5$ . From Figure 4 follows that  $\gamma_1(T)$  can be qualitatively described at  $T \ll T_c$  by

$$\gamma_1 \propto \exp(A/kT), \quad (1)$$

where  $A$  = activation energy. This finding agrees with  $\gamma_1(T)$ -measurements<sup>7</sup> as well as with measurements of the bulk viscosity<sup>5</sup>  $\eta(T)$  made with other polar liquid crystals. Like the elastic constants,  $\gamma_1$  also depends on the position of the alkenyl double bond. When disregarding for the moment differences of activation energies, Figure 4 shows that  $\gamma_1$  increases when shifting the double bond from 1  $\rightarrow$  3 (c.f.  $m_1$  and  $m_3$ ). Incorporating the ethane linkage into the rigid core causes  $\gamma_1$  to increase still further (c.f.  $m_3$  and  $m_5$ ). On the other hand a shift from position 1  $\rightarrow$  4 leads to a remarkable reduction of  $\gamma_1$  (c.f.  $m_1$  and  $m_4$ ).

For a direct comparison of single components, Figure 5 shows the temperature dependence of the rotational viscosity of the two 1-position alkenyls 3d<sub>1</sub>CP and 3d<sub>1</sub>CAP as well as  $\gamma_1(T)$  of the respective structurally related PCH5 and 5CAP. Also included in Figure 5 is K15.

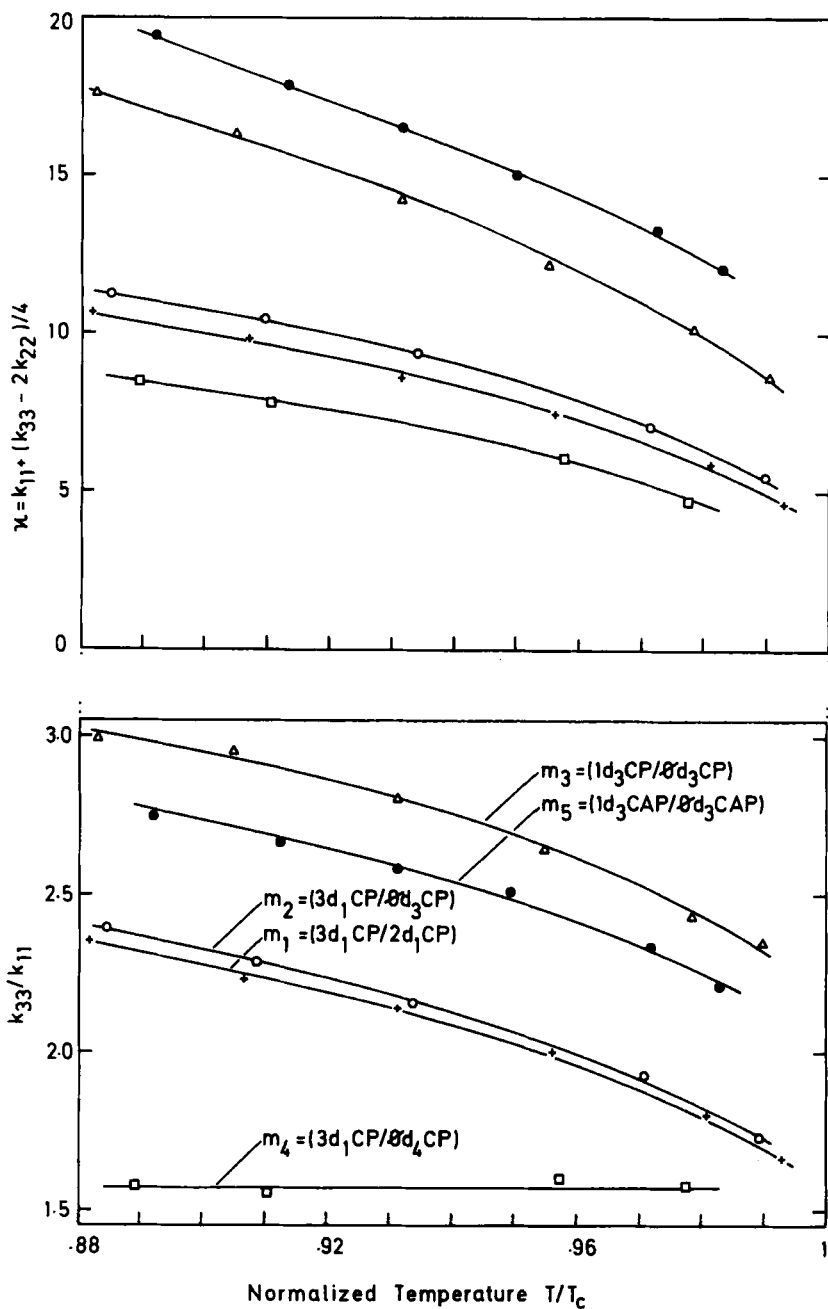


FIGURE 3 Temperature dependence of the elastic ratio  $k_{33}/k_{11}$  and of  $\kappa = k_{11} + (k_{33} - 2k_{22})/4$  of alkenyl mixtures  $m_1$ – $m_5$ .

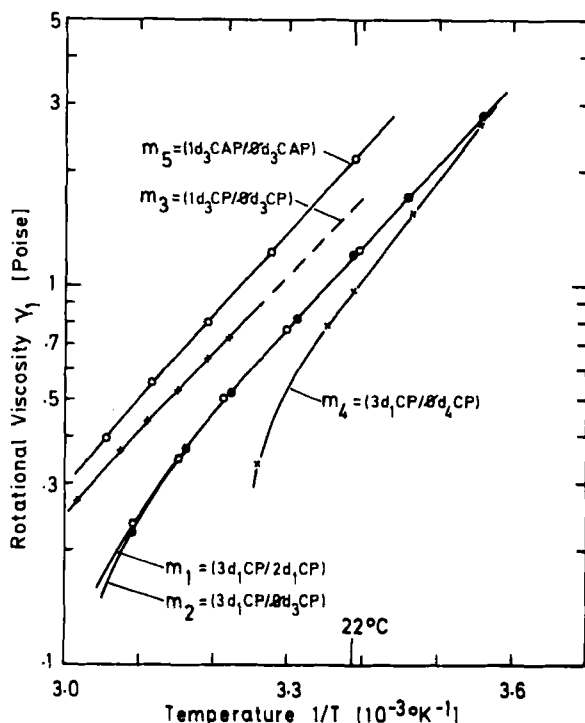


FIGURE 4 Temperature dependence of the rotational viscosities  $\gamma_1$  of alkenyl mixtures  $m_1$ – $m_5$ .

### 3. COMPARISONS BETWEEN ALKENYLS AND OTHER NEMATICS

#### 3.1. LC-material parameters and electro-optical performance of TN-LCDs

The electro-optical measurements in TN-LCDs were made at vertical light incidence in  $d = 8 \mu\text{m}$  spaced, polymer aligned, low bias tilt,  $\pi/4$ -twisted displays. The LCD-response times were measured at driving voltages  $V = 2.5 V_{10}(T)$ , where  $V_{10}(T)$  = optical threshold voltage at temperature  $T$  corresponding to 10% transmission;  $t_{\text{off}}$  = decay time corresponding to a change of transmission from 100%  $\rightarrow$  10% following the turn-off of  $V$ .

From relating numerically calculated electro-optical characteristics with LC-material parameters and from the performance of materials in TN-LCDs we have shown earlier<sup>1</sup> that the slope of the transmission

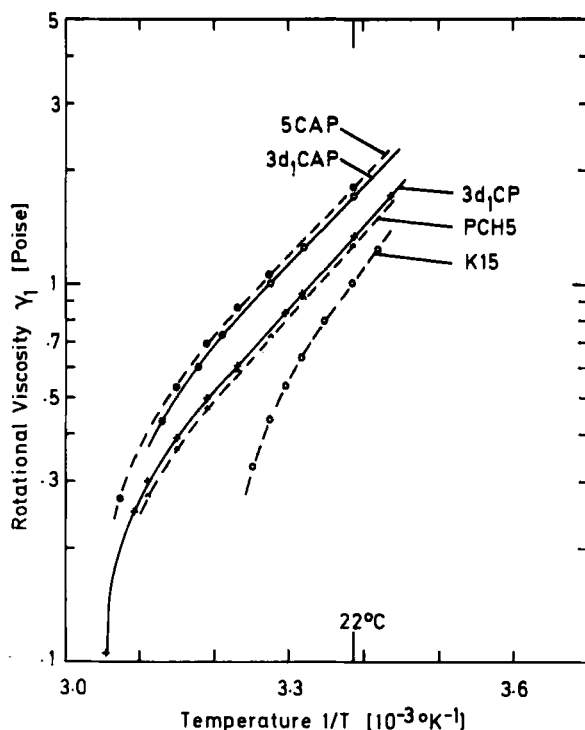


FIGURE 5 Temperature dependence of the rotational viscosities  $\gamma_1$  of alkenyl components 3d<sub>1</sub>CP, 3d<sub>1</sub>CAP and of reference compounds PCH5, 5CAP and K15.

characteristics of low bias tilt TN-LCDs can be approximated at vertical light incidence and around the second Mauguin transmission minimum by

$$p \simeq a + b \left( \frac{k_{33}}{k_{11}} - 1 \right) + c \left( \ln \frac{\Delta n d}{2\lambda} \right)^2. \quad (2)$$

The experimentally determined constants  $a$ ,  $b$  and  $c$  depend on the specific TN-LCDs used i.e. on the technology such as the surface aligning technique. For our display  $a = 0.119$ ,  $b = 0.035$  and  $c = 0.135$  hold. Approximation (2) shows that small elastic ratios  $k_{33}/k_{11}$  are most crucial for achieving small slope parameters  $p = (V_{50} - V_{10})/V_{10}$  which—according to  $N = [(p+1)^2 + 1]^2 / [(p+1)^2 - 1]^2$ —are a prerequisite to reach large multiplexing ratios  $N$ . Other material parameters like  $k_{22}/k_{11}$  (which should be large to lower  $p$ )<sup>15</sup> and  $\Delta\epsilon/\epsilon_{\perp}$  (which should be small in case of small optical path differ-

ences  $\Delta nd$ )<sup>15</sup> are—due to their minor importance at the second Mauguin minimum—neglected in (2).

Because of the increase of the select voltage with increasing multiplexing ratio, materials are required not only having steep electro-optical characteristics but also exhibiting optical thresholds low enough to remain CMOS-compatible. The optical threshold of TN-LCDs at vertical light incidence can be approximated by<sup>1,16</sup>

$$V_{10} \simeq V_{50} \left[ 0.88 - 0.024(k_{33}/k_{11} - 1) - 0.04 \left( \ln \frac{\Delta nd}{2\lambda} \right)^2 \right] \quad (3)$$

where,

$$V_{50} = V_c \left[ 2.044 - 1.044 / (k_{33}/k_{11} + 1) \right] \cdot \left[ 1 + 0.123 \{ (\Delta\epsilon/\epsilon_{\perp})^{0.6} - 1 \} \right] \cdot \left[ 1 + 0.132 \ln \frac{\Delta nd}{2\lambda} \right],$$

and the threshold for the mechanical deformation of the helical structure of the TN-LCD is

$$V_c = \pi [\kappa / \epsilon_0 \Delta\epsilon]^{1/2}.$$

From approximation (3) follows that both, the dielectric anisotropy  $\Delta\epsilon$  as well as the elastic expression  $\kappa$  essentially determine  $V_{10}$  of TN-LCSD.

Because of the similar  $\kappa$ -values of the so far most frequently used polar nematics<sup>1</sup> it was often possible to relate directly the differences among different decay times of TN-LCDs to the different viscosities of the LC-materials. However, with compounds such as alkenyls exhibiting large  $\kappa$ -variations this approach leads to wrong conclusions about the dynamics of TN-LCDs. Thus, if complex numerical calculations such as those of Berreman<sup>17</sup> are avoided, at least the heuristic expression derived by Jakeman and Raynes<sup>18</sup> which relates small angles of deformations of the nematic director to the decay time  $t_d$  of TN-LCDs should be used:

$$t_d \propto \gamma / \kappa \quad (4)$$

where  $\gamma$  is an undefined viscosity for which bulk viscosities  $\eta$ <sup>5,6</sup> and recently also rotational viscosities  $\gamma_1$ <sup>7</sup> were inserted. The small angle approximation (4) is not really applicable to the large director deformations corresponding to (practical) LCD turn-off times  $t_{off}$ <sup>7</sup>. All the

same it will be interesting to relate  $t_d$  of (4) qualitatively with  $\gamma_1$ ,  $\gamma_1/\kappa$  and  $t_{off}$ .

### 3.2. Material properties and structures

Table II summarizes the material properties of the alkenyl components and mixtures of Table I as well as those of the reference compounds. Comparisons of the elastic, dielectric and optical properties are made at constant reduced temperature ( $T_c - 10^\circ\text{C}$ ), whereas viscosities and viscosity related properties are compared at  $T = 22^\circ\text{C} = \text{constant}$ . The data belonging to ( $T_c - 10^\circ\text{C}$ ) in Table II are depicted in the upper line of the respective compound; the lower line refers to  $22^\circ\text{C}$ .

Except for the optical anisotropy  $\Delta n$  and the mesomorphic temperature range which are both larger in case of  $3d_1\text{CP}$ , a comparison between the 1-alkenyl  $3d_1\text{CP}$  and PCH5 shows that the two compounds are quite similar (Tab. I, II). Shifting the double bond from position 1  $\rightarrow$  3 causes—in analogy to mixtures  $m_1 \dots m_5$ — $\kappa$  to increase strongly.  $\Delta n$  of  $1d_3\text{CP}$  is about 30% larger than that of PCH5. The different  $\Delta n$ -values of  $1d_3\text{CP}$  and  $3d_1\text{CP}$  indicate that the angle of the double bonds parallel to the nematic director depends on bond position. From the data of the ethane linked components  $3d_1\text{CAP}$  and  $5\text{CAP}$  in Table II follows that the ethane linkage causes  $\kappa$  as well as  $k_{33}/k_{11}$  to increase compared with  $3d_1\text{CP}$  and PCH5.

From the similar data of the dioxane mixtures  $m_6$  and  $m_7$  in Table II and from the data of  $3d_1\text{CP}$  follows that the double bond in 1-position hardly affects the elastic or dielectric properties. However, in agreement with our earlier findings<sup>1</sup> the data of  $k_{33}/k_{11}$  of mixtures  $m_6$  and  $m_1$  show that heterocyclic rings in the rigid part of molecules lead to a reduction of  $k_{33}/k_{11}$ .

The striking dependence of  $k_{33}/k_{11}$  on alkenyl position led us to investigate semi-quantitatively whether rod-like and strain-free alkenyl conformations exist and whether the length/width ratio of the rods changes upon shifting the double bond. This was done with the Roche molecular modellings system (Roche Interactive Molecular Graphics RIMG)<sup>20</sup> designed to determine equilibrium structures and conformations of complex molecules based on inter- and intramolecular van der Waals interactions and conformational torsional potentials. To obtain the rod-like structures assumed by theory<sup>9,10</sup> we imposed the following boundary conditions: the strain-free conformations of the alkenyls have to fit into a cylindrically shaped frame in such a way that no unusual stress or strain bonding energies result.

TABLE II

Elastic constants  $k_{11}$ ,  $k_{22}$ ,  $k_{33}$ ,  $\kappa = k_{11} + (k_{33} - 2k_{22})/4$ , static dielectric constants  $\epsilon_{\perp}$ ,  $\Delta\epsilon = (\epsilon_{\parallel} - \epsilon_{\perp})$  and optical constants  $n_0$ ,  $\Delta n = (n_e - n_0)$  determined at the respective temperatures ( $T_c - 10^\circ\text{C}$ ) (upper lines) and  $T = 22^\circ\text{C}$  (bottom lines). The dot in the bottom line of 5CAP indicates that the data are extrapolated to  $22^\circ\text{C}$ .

LC	$k_{11}$	$k_{22}$	$k_{33}$	$k_3/k_1$	$\kappa$	$\epsilon_{\perp}$	$\Delta\epsilon$	$\Delta n$	$n_0$
3d <sub>1</sub> CP	6.22	3.90	13.4	2.13	7.5	5.70	10.94	0.116	1.490
	9.40	6.15	22.8	2.42	12.0	5.02	13.03	0.136	1.493
1d <sub>3</sub> CP	9.41	5.74	24.1	2.56	12.6	5.02	13.13	0.130	1.483
3d <sub>1</sub> CAP	9.18	5.28	18.5	2.02	11.2	4.96	10.48	0.118	1.486
	11.22	6.57	24.3	2.17	14.0	4.61	11.13	0.129	1.487
K15 (5B)	6.37	3.81	8.60	1.35	6.6	6.63	13.33	0.178	1.532
	7.12	4.09	9.82	1.38	7.5	6.46	13.82	0.185	1.533
PCH5 (5CP)	6.07	3.48	10.5	1.73	7.0	5.59	10.28	0.099	1.485
	8.98	4.73	18.3	2.03	11.2	4.85	12.22	0.119	1.487
5CAP	8.85	4.60	16.1	1.82	10.6	4.98	9.77	0.101	1.486
	• 12.05	6.65	24.0	1.99	14.7	4.40	10.80	0.116	1.483
$m_1 = (3d_1\text{CP}/2d_1\text{CP})$	5.65	3.42	10.7	1.90	6.6	5.77	11.62	0.117	1.492
	7.83	4.75	17.4	2.22	9.8	5.20	13.89	0.138	1.494
$m_2 = (3d_1\text{CP}/8d_3\text{CP})$	6.10	3.92	11.8	1.93	7.1	5.56	11.49	0.115	1.493
	8.20	5.22	18.7	2.28	10.3	5.00	13.57	0.135	1.495
$m_3 = (1d_3\text{CP}/8d_3\text{CP})$	8.08	4.65	20.7	2.56	10.9	5.01	12.38	0.127	1.487
	12.29	6.80	36.5	2.97	18.0	4.40	15.10	0.153	1.493
$m_4 = (3d_1\text{CP}/8d_4\text{CP})$	4.90	2.80	7.50	1.53	5.4	6.18	10.80	0.105	1.498
	5.52	3.20	8.60	1.56	6.1	6.03	11.23	0.108	1.500
$m_5 = (1d_3\text{CAP}/8d_3\text{CAP})$	0.25	5.95	24.3	2.37	13.4	4.64	11.74	0.122	1.485
	13.80	8.00	37.9	2.75	19.3	4.17	13.37	0.139	1.486
$m_6 = (4d_1\text{DP}/3d_1\text{DP})$	4.80	3.00	6.14	1.28	4.8	9.75	15.62	0.099	1.491
$m_7 = (4\text{DP}/5\text{DP})$	4.73	3.08	6.43	1.36	4.8	10.58	15.27	0.089	1.488
	5.88	3.99	8.41	1.43	6.0	9.99	17.06	0.100	1.487

The cylindrical frame was defined by the rod-shaped van der Waals volume resulting from the rotation of a tricyclic bicyclooctane structure around its long axis. At one end of the cylinder a benzene ring was attached which had favourably to coincide with the benzene ring P of the alkenyl fitted into the cylinder.

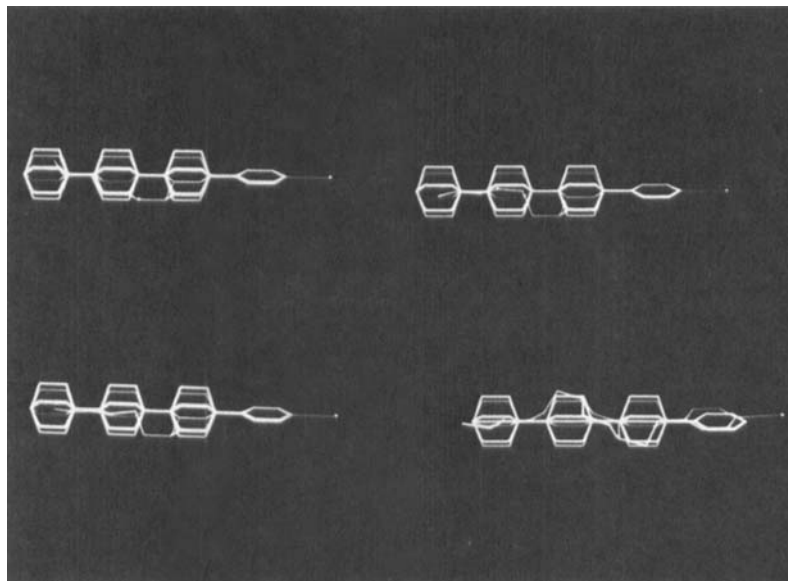


FIGURE 6 Energetically relaxed molecular conformations of polar alkenyls (red structures) fitted by molecular modelling into a cylindrically shaped bicyclooctane frame (blue-white structure) to which a benzene ring is attached on the right. The following alkenyls are fitted into the frame 4d<sub>1</sub>CP (upper left), 2d<sub>3</sub>CP (upper right), 1d<sub>4</sub>CP (lower left) and 2d<sub>3</sub>CAP (lower right). See Color Plate 1x located in the final volume of these Conference Proceedings.

Figure 6 shows the calculated equilibrium structures of 4d<sub>1</sub>CP, 2d<sub>3</sub>CP, 1d<sub>4</sub>CP and 2d<sub>3</sub>CAP (red molecules) in the rotationally symmetric bicyclooctane cylinder. The position of the alkenyl double bond is indicated with two red dots, the cyano end group pointing to the right (red dot connected to benzene ring). From Figure 6 follows that even the bulky ethane-linked alkenyl 2d<sub>3</sub>CAP fits well into the cylinder if a dislocation of its benzene ring from the benzene ring of the frame is allowed. The resulting strain-free conformations in Fig. 6 show that the length/width ratios of the directly linked alkenyls are—independently of the position of the double bond—identical, i.e.  $L/W = \text{constant}$ . Therefore, we see no reason to relate the constant length/width ratio  $L/W$  of alkenyls with the strongly different elastic ratios  $1.5 < k_{33}/k_{11} < 2.6$  of 3d<sub>1</sub>CP, 1d<sub>3</sub>CP and m<sub>4</sub> (Table II). Besides, although  $L/W$  of the rod formed by 1d<sub>3</sub>CAP increases due to the ethane linkage its  $k_{33}/k_{11}$  does not increase (Tab. II).

By analogy to the above, Figure 7 shows the long and short axis of the rod-shaped van der Waals radii of the strain-free conformation of



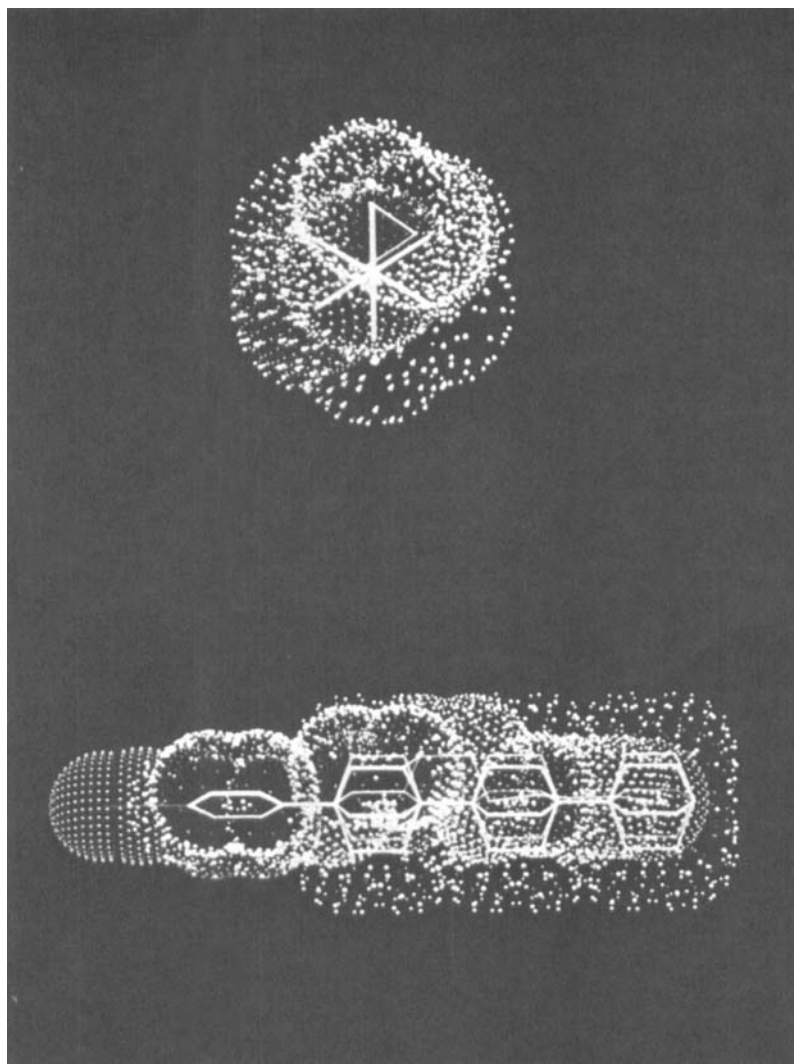


FIGURE 7 van der Waals radii of bicyclooctane cylinder frame (blue-white dots) incorporating  $2d_3CP$  (red dots). The lower picture shows the rod-shaped long cylinder axis whereas the upper part is a projection of the alkenyl side chain along the long cylinder axis showing its fit into the bicyclooctane frame. See Color Plate X located in the final volume of these Conference Proceedings.

$2d_3CP$  of Figure 6 within the bicyclooctane frame. Figure 7 shows that the rod-like van der Waals shapes of polar alkenyls indeed fit well into the cylindrically shaped bicyclooctane van der Waals frame.

**3.3. The dynamics of alkenyls**

From the rotational viscosities depicted in Figures 4 and 5 one would expect 1,4-alkenyl mixture  $m_4$  to exhibit a faster electro-optical response than either PCH5 or the 3-alkenyl mixture  $m_3$ . However, their visco-elastic ratios  $\alpha = \gamma_1/\kappa$  depicted in Figure 8 indicate that this is not the case. Figure 8 shows that not only the course of the temperature dependence of  $\gamma_1/\kappa$  changes compared with  $\gamma_1$  (Fig. 4) but also the respective order of increasing  $\gamma_1$  and  $\gamma_1/\kappa$ . Thus, although  $\gamma_1(m_4) < \gamma_1(\text{PCH5}) < \gamma_1(m_3)$  it follows from the  $\kappa$ -values of Figure 3 that  $\gamma_1/\kappa(m_4) > \gamma_1/\kappa(\text{PCH5}) > \gamma_1/\kappa(m_3)$ . Therefore, and provided approximation (4) holds,  $m_3$  is expected to exhibit considerably faster decay times than the less viscous mixture  $m_4$  or PCH5.

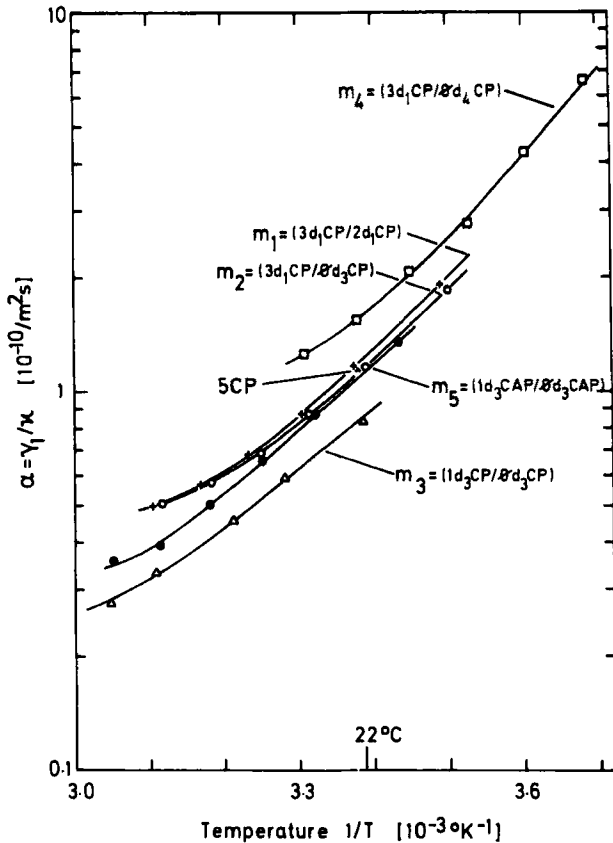


FIGURE 8 Temperature dependence of the visco-elastic ratio  $\gamma_1/\kappa$  of alkenyl mixtures  $m_1$ – $m_5$ . Also included is PCH5 (5CP).

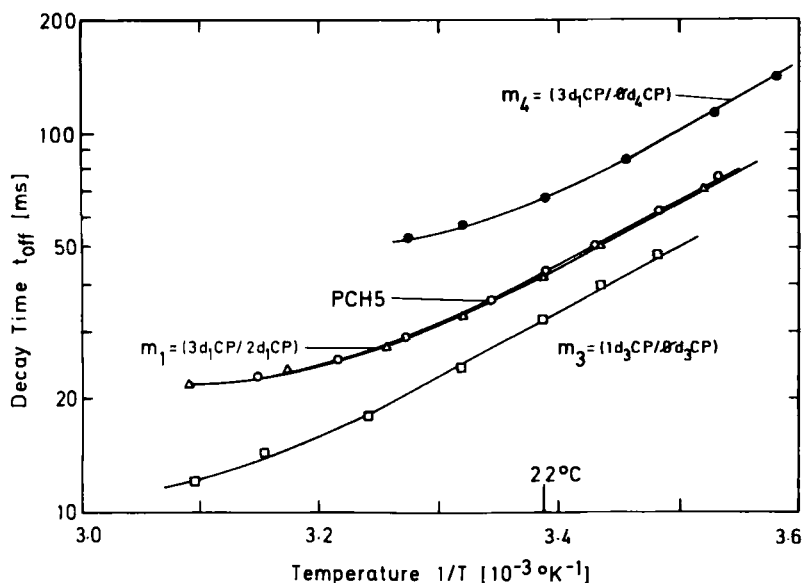


FIGURE 9 Temperature dependence of the decay time  $t_{\text{off}}$  of TN-LCDs comprising alkenyl mixtures  $m_1$ ,  $m_3$ ,  $m_4$  and PCH5 respectively.

Figure 9 shows that the activation energies of the decay times  $A(t_{\text{off}})$  at  $T \ll T_c$  are comparable to those of the visco-elastic ratios  $A(\gamma_1/\kappa)$  of Figure 8 but smaller than  $A(\gamma_1)$ . The data are summarized in Table III.

Moreover, the order of increasing  $t_{\text{off}}$  is the same as that found for  $\gamma_1/\kappa$  (Fig. 8 and 9). Thus, the simple approximation (4) can be used—together with  $\gamma_1/\kappa$ —to predict qualitatively the decay times of TN-LCDs at least over the rather small temperature ranges investigated here.

TABLE III

Activation energies  $A$  of the rotational viscosity  $\gamma_1$ , the visco-elastic ratio  $\gamma_1/\kappa$  and the TN-LCD decay time  $t_{\text{off}}$  (100%  $\rightarrow$  10%) at  $T \ll T_c$ .

	$A(\gamma_1)$ [eV]	$A(\gamma_1/\kappa)$ [eV]	$A(t_{\text{off}})$ [eV]
$m_4$	0.51	0.39	0.36
$m_1$	0.42	0.35	0.32
PCH5	0.43	0.35	0.32
$m_3$	0.41	0.32	0.32

TABLE IV

Rotational ( $\gamma_1$ ) and bulk viscosities ( $\eta$ ), activation energy  $A(\gamma_1)$  of  $\gamma_1$ , visco-elastic ratio  $\alpha = \gamma_1/\kappa$  as well as normalized visco-elastic ratios  $\alpha(\text{LC})/\alpha(5\text{CP})$  and TN-LCD decay times  $t_{\text{off}}(\text{LC})/t_{\text{off}}(5\text{CP})$  normalized with respect to PCH5.  $V_{10}$  = optical threshold voltage of TN-LCDs. All measurements made at 22°C.

LC	$\gamma_1$ [Poise]	$A(\gamma_1)$ [eV]	$\alpha = \frac{\gamma_1}{\kappa}$ [10 <sup>-10</sup> /m <sup>2</sup> s]	$\frac{\alpha(\text{LC})}{\alpha(5\text{CP})}$	$\eta$ [Poise]	$t_{\text{off}}$ [ms]	$\frac{t_{\text{off}}(\text{LC})}{t_{\text{off}}(5\text{CP})}$	$V_{10}$ [Volts]
3d <sub>1</sub> CP	1.34	.43	1.11	.97	.221	40	.93	1.58
3d <sub>1</sub> CAP	1.70	.41	1.21	1.06	.228	38	.88	1.89
K15 (5B)	1.01	.54	1.35	1.18	.263	55	1.28	1.13
PCH5 (5CP)	1.28	.43	1.14	1.00	.215	43	1.00	1.55
5CAP	1.80	.42	1.22	1.07	.224	43	1.00	2.00
$m_1 = (3d_1\text{CP}/2d_1\text{CP})$	1.21	.42	1.23	1.08	.228	42	.98	1.47
$m_2 = (3d_1\text{CP}/8d_3\text{CP})$	1.19	.42	1.15	1.01	.209	37	.86	1.62
$m_3 = (1d_3\text{CP}/8d_3\text{CP})$	1.50	.41	.83	.73	.190	32	.74	2.09
$m_4 = (3d_1\text{CP}/8d_4\text{CP})$	.97	.51	1.59	1.38	.278	67	1.56	1.13
$m_5 = (1d_3\text{CAP}/8d_3\text{CAP})$	2.15	.43	1.11	.98	-	29	.67	2.29

Table IV shows measurements made at 22°C of the rotational and bulk viscosities  $\gamma_1$  and  $\eta$  of alkenyls and reference compounds. Also shown are their activation energies  $A(\gamma_1)$ , the viscoelastic ratios, the decay times and the optical threshold voltages. Because of their comparable dielectric anisotropies (Tab. II) and in agreement with approximation (3), the compounds with large  $\kappa$ -values also exhibit high optical thresholds  $V_{10}$  (Tab. IV). Table IV shows that  $\gamma_1$  of  $m_4$  and K15 are considerably lower than those of  $m_3$  or PCH5. However, the decay times of  $m_4$  and K15 are—due to their large visco-elastic ratios—more than 30% larger than  $t_{\text{off}}$  (PCH5). On the other hand the response of the 3-alkenyl mixture  $m_3$  is 26% faster than that of PCH5 (Tab. IV, Fig. 9). From the  $\kappa$ -values in Table II and the bulk viscosities  $\eta$  depicted in Table IV follows that  $\eta/\kappa$  and  $t_{\text{off}}$  correlate not as well as  $\gamma_1/\kappa$  and  $t_{\text{off}}$ . The discrepancy becomes most pronounced when comparing the low  $\gamma_1$  compounds K15 and  $m_4$  with the other compounds in Table IV. This finding confirms our earlier results obtained with other LC-classes<sup>7</sup>. From the above follows that even qualitative electro-optical response considerations cannot be based on viscosity data alone, the elastic properties must be considered too.

#### 4. CONCLUSIONS

From investigations into the dielectric, birefringence, viscous, electro-optical and all three elastic constants we have shown that the new, low viscous polar nematic alkenyls synthesized in our laboratories cover an unusually wide range of elastic properties rendering them applicable in LCDs requiring fast response as well as high multiplexability. With sterically and dielectrically comparable representatives of five different alkenyl classes it was found that the elastic ratio  $k_{33}/k_{11}$  as well as the elastic expression  $\kappa = k_{11} + (k_{33} - 2k_{22})/4$  strongly depend on the position of the alkenyl double bond in the hydrocarbon side chain. By means of molecular modelling, the rod-like van der Waals structure of directly—as well as ethane linked alkenyls was verified and shown that the length/width ratio  $L/W$  of the rods is constant. On the other hand  $k_{33}/k_{11} \neq \text{constant}$ . Therefore, and since steric considerations alone do not suggest the postulation of hypothetical steric units either whose  $L/W$ -ratio may (or may not) change, we conclude that hard-rod models that disregard specific molecular interactions and which imply  $L/W \propto k_{33}/k_{11}$  are inadequate.

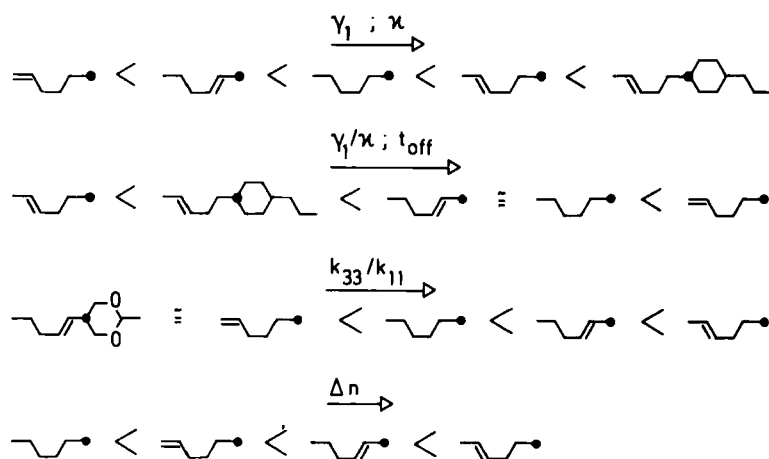


TABLE V

Summary and schematic representation of the influence of alkenyl double bond position on  $\gamma_1$ ,  $\kappa$ ,  $\gamma_1/\kappa$ ,  $t_{off}$ ,  $k_{33}/k_{11}$  and  $\Delta n$ . Directly linked alkenyls with PCH-core are depicted with their alkenyl side chains only. In case of the ethane-linked (Id<sub>3</sub>CAP) and the dioxane (3d<sub>1</sub>DP) alkenyl, the rings attached to the alkenyl side chain are included. Also included in the schematic is PCH5 (saturated chain).

quate to describe the elastic ratios of nematics. Because of the low rotational viscosities and the large  $\kappa$ -values of 3-alkenyls, low visco-elastic ratios  $\gamma_1/\kappa$  result. As a consequence, 3-alkenyls exhibit response times in TN-LCDs that are  $\sim 30\%$  shorter than those of comparable PCHs while their optical anisotropy  $\Delta n$  is larger than  $\Delta n$  of PCHs. By analogy with our earlier findings with other liquid crystal classes, rigid cores of alkenyls comprising heterocyclic rings are shown to exhibit lower elastic ratios  $k_{33}/k_{11}$  than non-heterocyclic compounds.

Table V summarizes schematically our findings of the positional-dependent influence of the alkenyl double bond on  $k_{33}/k_{11}$ ,  $\kappa$ ,  $\gamma_1$ ,  $\gamma_1/\kappa$  and  $\Delta n$ . Also shown is the influence of the dioxane ring on  $k_{33}/k_{11}$  and the effect of the ethane linkage in the 'rigid' core. Due to the dependence of  $\Delta n$  on double bond position, the average angle of the bond with respect to the nematic director is—contrary to the schematic in Table V—position dependent.

### Acknowledgements

We wish to thank Dr. K. Mueller for performing the molecular modelling with the Roche Interactive Molecular Graphics system. We also gratefully acknowledge the assistance of B. Blöchliger, A. Germann, V. Kannookadan and J. Reichhardt in the experimental work.

### References

1. M. Schadt and P. R. Gerber, *Z. Naturforsch.* **37a**, 165 (1982).
2. W. H. de Jeu and W. A. P. Claassen, *J. Chem. Phys.* **67**, 3705 (1977).
3. Hp. Schad, G. Baur and G. Meier, *J. Chem. Phys.* **70**, 2770 (1979).
4. R. Eidenschink, D. Erdmann, J. Krause and L. Pohl, *Angew. Chem.* **89**, 103 (1977).
5. M. Schadt and F. Mueller, *Rev. Phys. Appliquée* **14**, 265 (1979).
6. J. Constant and E. P. Raynes, *Mol. Cryst. Liq. Cryst.* **62**, 115 (1980).
7. P. R. Gerber and M. Schadt, *Z. Naturforsch.* **37a**, 179 (1982).
8. W. Maier and A. Saupe, *Z. Naturforsch.* **14a**, 882 (1959).
9. R. G. Priest, *Phys. Rev.* **A7**, 720 (1973).
10. J. P. Straley, *Phys. Rev.* **A8**, 2181 (1973).
11. F. Leenhouts and A. J. Dekker, *Mol. Cryst. Liq. Cryst.* **74**, 1956 (1981).
12. N. Carr, G. W. Gray and D. G. McDonnell, *Mol. Cryst. Liq. Cryst.* **97**, 13 (1983).
13. G. W. Gray, K. J. Harrison and J. A. Nash, *Electron. Lett.* **9**, 98 (1974).
14. H. M. Vorbroth, S. Deresch, H. Kresse, A. Wiegeleben, D. Demus and H. Zashcke, *J. Prakt. Chem.* **323**, 902 (1981).
15. G. Baur, *Mol. Cryst. Liq. Cryst.* **63**, 45 (1980).
16. M. Schadt, *Mol. Cryst. Liq. Cryst.* **89**, 77 (1982).
17. D. W. Berreman, *J. Appl. Phys.* **46**, 3746 (1975).
18. E. Jakeman and E. P. Raynes, *Phys. Lett.* **A39**, 69 (1972).
19. H. Gruler, *Z. Naturforsch.* **28a**, 474 (1973).
20. K. Mueller, *Chimia* **38**, 249 (1984).